Journal of Power Sources 243 (2013) 494–498

Contents lists available at SciVerse ScienceDirect

Journal of Power Sources

journal homepage: www.elsevier.com/locate/jpowsour

Short communication

Synthesis of FeOF using roll-quenching method and the cathode properties for lithium-ion battery

Ayuko Kitajou [a], Hideyuki Komatsu [b], Rintarou Nagano [c], Shigeto Okada [d,*]

[a] Research and Education Center of Carbon Resources, Kyushu University, 6-1 Kasuga-koen, Kasuga 816-8580, Japan
[b] Graduate School of Integrated Frontier Sciences, Kyushu University, 6-1 Kasuga-koen, Kasuga 816-8580, Japan
[c] Interdisciplinary Graduate School of Engineering Sciences, Kyushu University, 6-1 Kasuga-koen, Kasuga 816-8580, Japan
[d] Institute for Materials Chemistry and Engineering, Kyushu University, 6-1 Kasuga-koen, Kasuga 816-8580, Japan

HIGHLIGHTS

- Rutile-type FeOF can be quickly synthesized in 1 min by the roll-quenching method.
- The obtained FeOF has exceedingly high energy density about 500 mAh g^{-1}.
- Although it is the conversion-type cathode, the cyclability was relatively good.

ARTICLE INFO

Article history:
Received 15 February 2013
Received in revised form
9 June 2013
Accepted 10 June 2013
Available online 18 June 2013

Keywords:
FeOF
Rutile
Roll-quenching method
Conversion reaction

ABSTRACT

Rutile-type FeOF is a promising cathode for lithium-ion batteries, because it has a relatively large theoretical capacity of 885 mAh g^{-1} in eco-friendly iron-based cathodes. Although it is difficult to synthesize by conventional solid-state synthesis methods, it can be quickly synthesized by the roll-quenching method. The quick synthesis method is suitable to reduce the produce cost, but also to avoid the fluorine gas release during synthesis procedure. The obtained FeOF by roll-quenching method has kept some crystallinities, and provides a large discharge capacity (900 mAh g^{-1}) between 0.7 and 4.0 V. The charge and discharge reaction mechanism was investigated by structural analyses.

1. Introduction

The demands for Li-ion batteries have been increasing in recent years due to their wide application to electric power storage for electric vehicles and small electric devices. Li-ion batteries constitute the current state of the art in high-energy-density rechargeable energy storage cells. Further advances in energy density have been limited by the energy density of their cathodes. The insertion-type cathodes of commercially available Li-ion batteries generally consist of lithium 3*d*-transition metal oxides such as $LiCoO_2$, $LiMn_2O_4$, and $LiFePO_4$. In many cases, the voltage is relatively high, but the specific capacities are not so large, because they are limited to a 1Li insertion/extraction based on 1 steep redox reaction such as Co^{3+}/Co^{4+}. On the other hand, the conversion-type electrodes can utilize all of the valence change between ionic and metallic state of cation of the electrode active material with breakdown of the initial crystal structure as follows;

$$nmLi^{+} + nme^{-} + MX_m \leftrightarrows mLi_nX + M^0 \quad (1)$$

where M = Fe, Co, Ni, Cu etc., and X = S^{2-}, O^{2-}, F^{-}, etc.

Reversible conversion reaction, which is denoted above have been demonstrated with metal sulfides [1,2], oxides [3], and finally fluorides [4–7]. Here, the idea to exploit metal fluorides as the conversion-type cathode arises from the ability to generate high voltage and large capacity. Both of these attributes come as a direct result of the large electro-negativity and small electrochemical equivalent of fluorine. In particular, FeF_3 cathode showed a larger discharge capacity for the insertion reaction of about 200 mAh g^{-1} at approximately 3.3 V vs. Li metal with a mixture of ethylene carbonate (EC) and dimethyl carbonate (DMC) dissolving with

* Corresponding author. Tel./fax: +81 92 583 7841.
E-mail addresses: s-okada@cm.kyushu-u.ac.jp, s-okada@mx3.canvas.ne.jp (S. Okada).

0378-7753/$ – see front matter © 2013 Elsevier B.V. All rights reserved.
http://dx.doi.org/10.1016/j.jpowsour.2013.06.053

1 mol dm^{-3} $LiPF_6$, which corresponds to 99% of the theoretical specific capacity (238 mAh g^{-1}) based on the FeF_3 content [4]. Furthermore, the theoretical capacity of FeF_3 based on a complete 3 Li conversion reaction can be estimated with 712 mAh g^{-1}. Actually, FeF_3-based nanocomposites showed that a reversible specific capacity over 600 mAh g^{-1} was realized at an average voltage of 2.2 V at 70 °C [5]. However, FeF_3-based nanocomposites using conversion reactions showed poor cyclability.

Moving from iron fluorides into iron oxyfluoride, one can expect improvement of the cyclability and conductivity by covalent M–O bonds introduced into the highly ionic fluoride structure. In addition, iron oxyfluoride, FeOF, has also been proposed as a new candidate with larger theoretical capacity than that of FeF_2 or FeF_3 as follows:

$FeF_2 + 2Li \rightleftarrows Fe + 2LiF$ (theoretical capacity: 571 mAh g^{-1})

$FeF_3 + 3Li \rightleftarrows Fe + 3LiF$ (theoretical capacity: 712 mAh g^{-1})

$FeOF + 3Li \rightleftarrows Fe + LiF + Li_2O$ (theoretical capacity: 885 mAh g^{-1})

In order to investigate the impact of introducing oxygen into the fluoride structure on electrochemical performance, we tried to synthesize iron oxyfluoride compounds. F. J. Brink et al. has previously reported the solid-state synthesis at elevated temperatures (950 °C, 24 h) of FeO_xF_{2-x} solid solutions utilizing FeF_3 and Fe_2O_3 precursors [8]. Moreover, N. Pereira and co-authors [9] reported carbon-iron oxyfluoride nanocomposites (FeOF/C) synthesized using a solution process. The discharge capacity of FeOF/C was 430 mAh g^{-1}, which corresponded to 48.6% of the theoretical capacity based on the 3 Li reaction per FeOF (885 mAh g^{-1}). However, it is difficult to synthesize the uniform single phase by conventional solid-state or solution-process synthesis. In particular, in order to decrease the volatilization amount of fluorine in FeOF, it is necessary to shorten the synthesis duration at elevated temperature.

In this work, the roll-quenching method was tried for quick FeOF synthesis. In addition, to examine the cathode properties of the obtained FeOF, and to determine the discharge reaction mechanism between Li and FeOF, the *k* local structure and crystal structure changes during the discharge reaction were investigated by synchrotron-based X-ray absorption spectroscopy (XAS), X-ray diffraction (XRD) measurement and X-ray photoelectron spectroscopy (XPS).

2. Experimental

2.1. Synthesis and electrochemical properties of FeOF

FeOF was prepared from a stoichiometric mixture of FeF_3 (Soekawa Chemical Co., Ltd.) and Fe_2O_3 (Sigma–Aldrich) with a molar ratio of FeF_3:Fe_2O_3 = 2.33:1. The mixture was ground in an Ar-filled glove box and placed in a silica-covered Pt tube. The Pt and silica tubes have a small hole of 1 mm in diameter at the bottom for injecting the melted sample into a single copper roller. In the roll-quenching machine (Harddays Co., Ltd.), the powder sample was heated by the joule heat of the induction current in the Pt tube. After heating to over 1000 °C for 40 s, high-pressure Ar gas was injected into the melted mixture, which was quenched onto a single copper roller with rotation at 2000 rpm in an Ar atmosphere. Flake-like quenched samples were collected in the Ar chamber.

The 70 wt. % obtained FeOF powder was dry-ball-milled with 25 wt. % acetylene black (AB, Denki Kagaku Co., Ltd.) in Ar. Cathodes were prepared by mixing the FeOF/C composite powder with a 5 wt. % PVDF binder (Kureha Corp.) in *N*-methylpyrrolidinone. The slurry was coated on aluminum foil and dried at 80 °C until the solvent had evaporated completely. The electrochemical performance of the FeOF was evaluated with a 2032 coin-type cell using a non-aqueous electrolyte (1 M $LiPF_6$/EC:DMC = 1:1 in volume, Kishida Chemical Co., Ltd.) and a polypropylene separator (Celgard 3501) against lithium metal (Honjo Metal Co., Ltd.). All the cells were assembled in an Ar-filled glove box. The charge–discharge measurement was performed in galvanostatic mode at a rate of 10 mA g^{-1} (0.015 C:1 C rate corresponds to a current rate of 885 mA g^{-1}). The test temperature was 25 °C. The cathode pellets were carefully taken out from the cells in the Ar-filled glove box, washed, immersed in DMC for one night to remove the electrolyte. Then, they were dried prior to being set in Ar-filled transfer vessel for XPS. In the case of XRD and XAFS measurements, Ar-filled sample folders were used, respectively.

2.2. Physical characterization of FeOF

The characterizations of the obtained FeOF powder and pellets after the charge or discharge processes were carried out with an X-ray powder diffractometer (XRD, 50 kV and 300 mA, Cu-Kα, Rigaku TTRIII). The XRD data for the pellet samples were taken under Ar atmosphere to avoid the oxidation of the bivalent iron in air. X-ray photoelectron spectroscopy (XPS) was carried out with JPS-9010 (JEOL Ltd.) using focused monochromatized Mg Kα radiation ($h\nu$ = 1253.6 eV). X-ray absorption measurements of the iron K-edge using synchrotron radiation were carried out at room temperature at beam line BL11 of Saga Light Source using a double Si(1 1 1) monochromator. The X-ray adsorption near edge structure (XANES) and the X-ray absorption fine structure (EXAFS) were measured. The thickness of the cathodes allowed the transmission mode measurements (Fe K-edge). The composition of the obtained FeOF was determined using an atomic adsorption spectrophotometer (AAS, Hitachi Z-2300) and Ion Chromatography (IC, TOSHO IC-2001), following the powder dissolving in the mixture of 30 wt% H_2O_2 and conc. HCl.

3. Results and discussion

3.1. Characterization of obtained FeOF

The crystal structure of the obtained FeOF was characterized with XRD, as shown in Fig. 1. The obtained FeOF by roll-quench method has higher crystallinity than that by ion exchanged and liquid-state [9]. The determined composition by AAS and IC was $FeO_{1.1\pm1}F_{0.97}$. The few deficiency of fluorine was caused by the stronger volatility of the fluorine than oxygen. It was able to be indexed as a tetragonal structure with space group $P4_2/mnm$, and a small amount of the starting material, FeF_3, remained as an impurity. While the lattice constants of ICDD No. 018-0648 were $a = b = 4.65$ Å and $c = 3.05$ Å, those of the obtained FeOF were $a = b = 4.67$ Å and $c = 3.10$ Å. It suggests that the axis of the obtained FeOF was extended beyond that of the reported axis of FeOF by rapidly cooling from 1000 °C to room temperature.

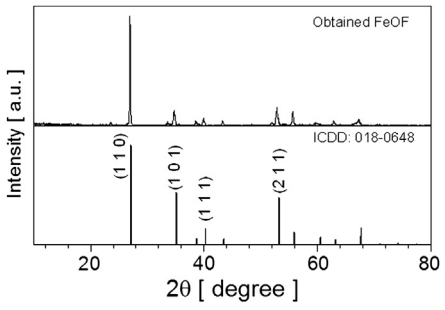

Fig. 1. X-Ray diffraction patterns for obtained FeOF.

3.2. The electrochemical property for FeOF vs. Li cell

Fig. 2 shows the initial discharge (Li^+ insertion) and charge (Li^+ extraction) curves of the obtained FeOF at a rate of 10 mA g^{-1}. During the first discharge process, the cell voltage gradually decreased through inflection points at around 2.6, 1.8 and 0.9 V. The first discharge capacity was 900 mAh g^{-1} down to 0.7 V, which almost corresponds to the theoretical capacity based on the 3 Li^+ conversion reaction (885 mAh g^{-1}). During the first charge process, the first charge capacity was 680 mAh g^{-1}, and there was a large polarization between the discharge and charge voltage profiles indicating irreversible transformation. It suggests that the discharge capacity of FeOF included a conversion reaction to Fe^0. In the case of FeF_3, such conversion reaction was also observed below 2 V in the discharge process. Fig. 3 shows the cyclability of the obtained FeOF at various voltage ranges. The first discharge capacities down to 2.0 V were 192 mAh g^{-1} and it was 180 mAh g^{-1} even after 30 cycles. By contrast, in the case of deeper cycle between 1.3 and 4.0 V, the first discharge capacity increased more than twice, which corresponds to 60% of the theoretical capacity based on the 3 Li conversion reaction. Although the irreversible capacity at first cycle was ca. 50 mAh g^{-1}, the cyclability efficiency was not so bad. The cycling efficiency of FeOF between 1.3 and 4.0 V was a 70.9%. For comparison, a FeF_3 between 1.3 and 4.5 V [5] and a FeF_2 between 1.5 and 4.5 V [9] exhibited a 29.2% and a 40–50% cycling efficiency, respectively. On the other hand, when the voltage range extended to 0.7 and 4.0 V, the cyclability of Li/FeOF cell was deteriorated within a few cycles, as shown in Fig. 3. It suggests the drastic change in the crystal structure and/or cell volume of FeOF around 1.3 V.

The discharge rate capability of FeOF between 1.3 and 4.0 V (Fig. 4) was studied with various currents from 10 mA g^{-1} (0.015 C rate) to 72 mA g^{-1} (0.11 C rate). The initial discharge capacity of FeOF vs. Li remained 350 mAh g^{-1} even at a rate of 72 mA g^{-1}. Moreover, the obtained FeOF had a good cyclability even in the study involving the conversion reaction cyclability at the rate of 60 mA g^{-1}, and the discharge capacity after 30 cycles remained ca. 300 mAh g^{-1} (Fig. 5). The energy density of the FeOF at rate of 10 mA g^{-1} was 1100 mWh g^{-1}, and it was almost twice of that of $LiFePO_4$.

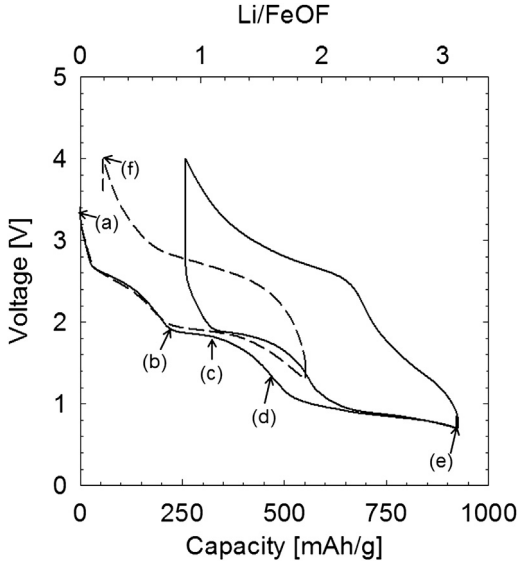

Fig. 2. Initial and second cycle profiles of FeOF vs. Li cell at a rate of 10 mA g^{-1}. The straight line shows the cycle profile between 0.7 and 4.0 V and the broken line shows the cycle profile between 1.3 and 4.0 V, respectively.

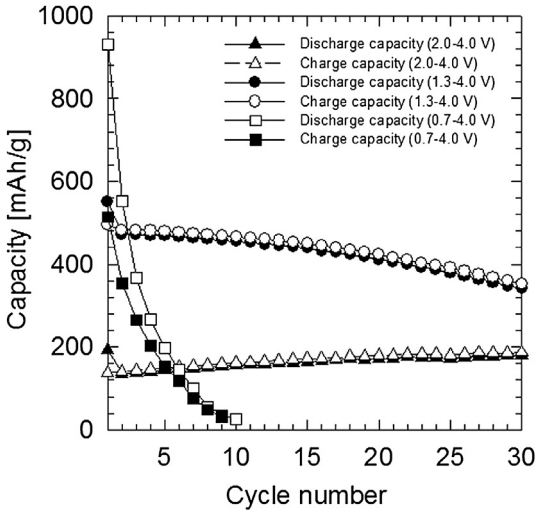

Fig. 3. Cyclability for FeOF against Li.

3.3. Structure change for FeOF during the discharge–charge process

Fig. 6 shows the near-edge X-ray absorption spectra of cathode pellets at (a) the initial FeOF pellet and discharged pellets down to (b) 2.0 V, (c) 1.8 V, (d) 1.3 V, (e) 0.7 V and metallic iron as a reference. Notably, the Fe K-edge position was shifted to 7112 eV from 7113 eV, when the discharge reaction progressed to 2.0 V from the initial state. In the discharge reactions at less than 2.0 V, the Fe K-edge position was shifted to still lower energy. Moreover, the small pre-edge feature near 7112 eV changed, depending on the lithium content per FeOF. This pre-edge feature corresponds to $1s \rightarrow 3d$ transitions, which are dipole forbidden in octahedral symmetry. Therefore, the strength reflects that the symmetry decreases with deeper discharge reaction than 1 Li per FeOF. At the discharge region below 2.0 V, the pre-edge feature approaches that of metallic iron. These results suggested that the oxidation state of iron changed from Fe^{3+} to Fe^{2+} down to 2.0 V, and that the oxidation state of Fe changed from Fe^{2+} to Fe^0 in the discharge reactions below 2.0 V.

The Fe 2p XPS peaks of FeOF were analyzed to examine the oxidation states during charge or discharge process. Fig. 7 shows the Fe 2p spectra of (a) the initial FeOF pellet and discharged pellets

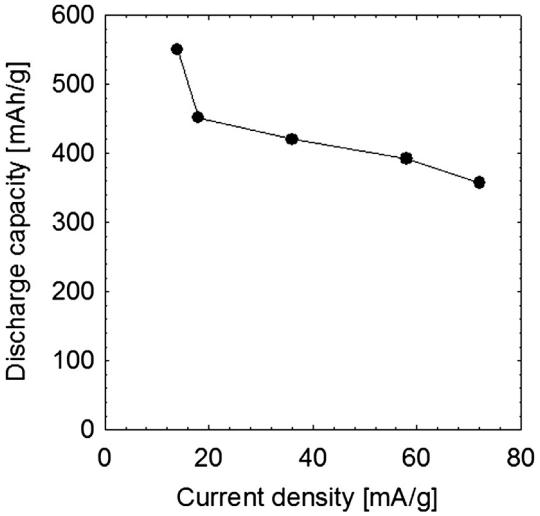

Fig. 4. Discharge rate capability of FeOF between 1.3 and 4.0 V against Li.

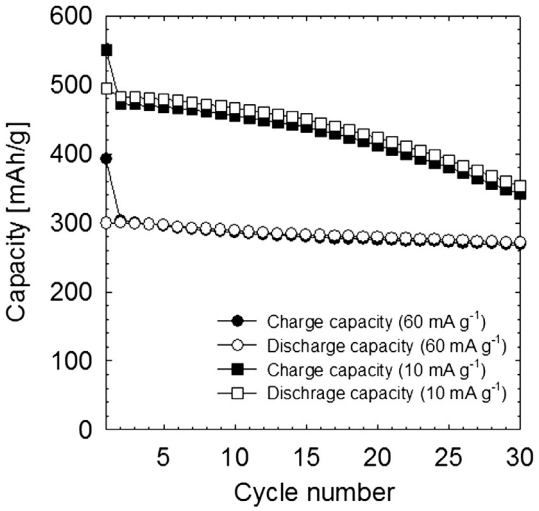

Fig. 5. Cyclability of FeOF between 1.3 and 4.0 V against Li. The current densities were 10 mA g^{-1} and 60 mA g^{-1}, respectively.

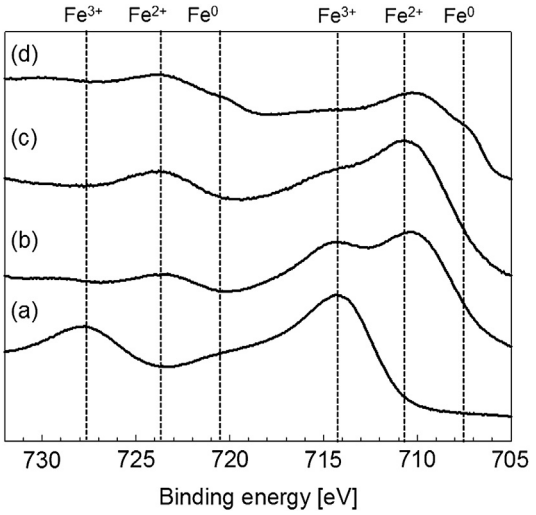

Fig. 7. XPS spectra of FeOF cathode pellets during the first discharge/charge cycle; (a) initial FeOF state, (b) discharged pellet down to 2.0 V, (c) 1.8 V and (d) 1.3 V, respectively.

down to (b) 2.0 V, (c) 1.8 V and (d) 1.3 V, respectively. The Fe^{2+} spectrum consisted of two peaks due to spin-orbit coupling of Fe $2p_{3/2}$ and $2p_{1/2}$. The $2p_{3/2}$ and $2p_{1/2}$ peaks of Fe^{2+} locate at 710.8 and 723.9 eV, respectively. For Fe^{3+}, the $2p_{3/2}$ and $2p_{1/2}$ peaks shift to 713.9 and 727.6 eV, and the $2p_{3/2}$ and $2p_{1/2}$ peaks for Fe^0 shift to 707.5 and 720.2 eV [10]. The obtained XPS spectra of several pellets show that the iron oxidation state was changed from Fe^{3+} to Fe^{2+} down to 2.0 V, while it changed from Fe^{2+} to Fe^0 less than 1.3 V.

Fig. 8 compares the XRD profiles of cathode pellets at (a) the initial FeOF, discharged down to (b) 2.0 V, (c) 1.8 V, (d) 1.3 V and (e) 0.7 V, (f) charged pellet up to 4.0 V after discharge down to 1.3 V, respectively. The main XRD peaks of (1 1 0) and (2 1 1) in the discharged pellet down to 2.0 V shifted to lower angles, while the diffraction peak intensities at 42°and 62°increased with discharge down to 1.8 V. The increase of FeOF unit cell dimensions suggest that discharge reaction occurring above 2.0 V is associated with lithium insertion into the FeOF structure. The lattice constant of FeOF down to 2.0 V were $a = b = 4.75$ Å and $c = 3.26$ Å, respectively. But after discharge down to 1.8 V, additional diffraction peaks were observed at 43° and 62°. The similar intermediate phase has also been detected as cubic Li–Fe–O phase by N. Pereira [9]. The appearance of this Li–Fe–O intermediate phase means the start of FeOF conversion reaction with LiF generation below 1.8 V. Actually, LiF and Fe diffraction peaks around 45° and 65° can be observed below 1.3 V in Fig. 8(d) and (e). This result suggests that the conversion of FeOF occurred within the 0.7–1.8 V regions with the reduction of Fe^{2+} into Fe metal. On the other hand, Fig. 8 shows the XRD profile of cathode pellets upon recharging to 4.0 V after first discharge down to 1.3 V. The XRD pattern cannot be

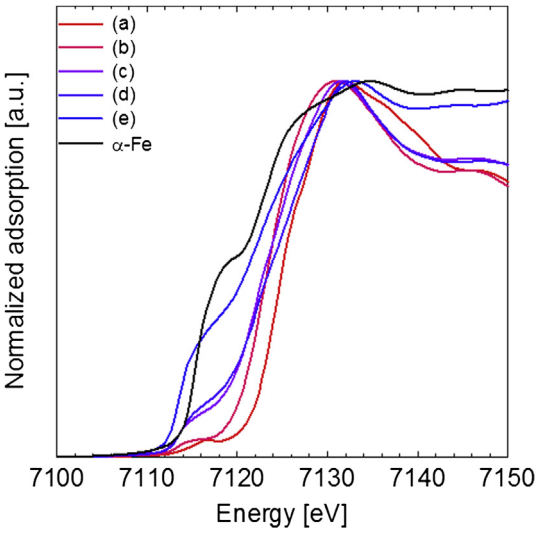

Fig. 6. *Ex-situ* XANES spectra of Fe in FeOF cathode pellets during the first discharge/charge cycle; (a) initial FeOF state, (b) discharged pellet down to 2.0 V, (c) 1.8 V, (d) 1.3 V and (e) 0.7 V, respectively.

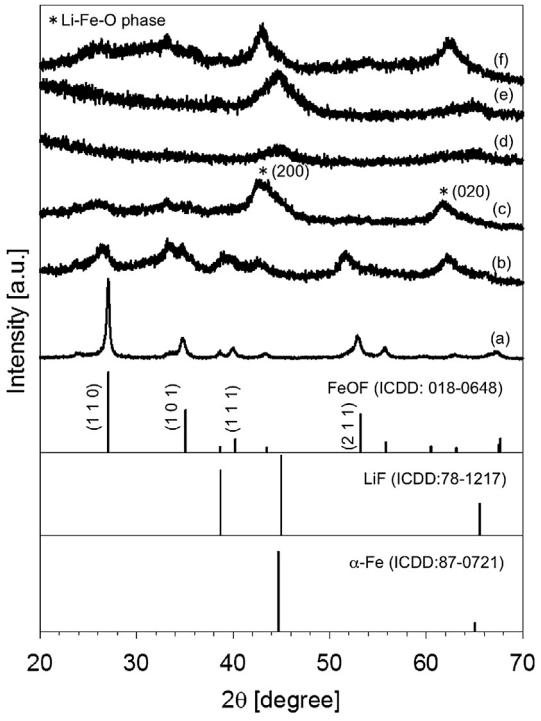

Fig. 8. *Ex-situ* XRD profile of FeOF cathode pellets during the first discharge/charge cycle; (a) initial FeOF state, (b) discharged pellet down to 2.0 V, (c) 1.8 V, (d) 1.3 V and (e) 0.7 V, respectively. In addition, (f) shows 4.0 V charged pellet after discharge down to 1.3 V.

indexed as the initial FeOF structure, but the Li_xFeOF structure, which changed to another crystal system at the discharge reaction down to 1.8 V was maintained. The position of XRD peaks shifted to a higher angle than that at 1.8 V. Therefore, we supposed that lithium was inserted/extracted into a changed Li_xFeOF structure.

Fig. 9 shows the Fourier transformation of the $\chi(k) \times k^3$ functions for FeOF cathode pellets in *R* space, where *R* is the uncorrected radius of the nearest-neighbor shells. The sampling points of the FeOF cathode pellets were the initial FeOF, discharged down to 2.0 V, 1.8 V, 1.3 V and 0.7 V, respectively. The peak positions in the Fourier-transformed $\chi(k) \times k^3$ function depends on the real radius *r* of the scattering shells around the X-ray absorbing atom. Therefore, the first peak of the Fourier-transformed $\chi(k) \times k^3$ functions in the initial FeOF cathode pellet is due to the scattering of the outgoing electron wave at the first oxygen and fluoride shell. The second peak shows the Fe–Fe bond in the FeOF structure. The peak feature of initial FeOF was maintained during discharge down to 2.0 V; however, that is changed to another peak feature below 2.0 V. From this result, we can conclude that the discharge reaction down to 2.0 V is an insertion reaction in which lithium is inserted into the initial FeOF structure, while the local structure around Fe changes into another symmetrical system by the deeper discharge reaction below 2.0 V. The average bond length between Fe and O(F) can be estimated 1.95–2.0 Å in FeOF with $P4_2/mnm$. On the other hand, the sum of the ion radius of 6 coordinated high spin Fe^{3+} cation and O^{2-}(F^-) anion is 1.94–2.01 Å. This coincidence suggests that Fe^{3+} anions are located at octahedral sites surrounded with 6 O^{2-} anions in FeOF. Generally, the *R* value tends to become smaller than the true bond length, because of the phase shift effect of photoelectron wave by the potential well forming around atoms. According to this influence, the *R* value of the first shell of initial FeOF in Fig. 9 can be considered to be consistent with the bond length of Fe^{3+}–O^{2-}.

However, the peak of the Fourier-transformed $\chi(k) \times k^3$ functions after discharge down to 1.8 V was changed and it showed a similar peak feature to the FeO standard sample. As mentioned above, the intermediate phase at 1.8 V may correspond to the cubic Li–Fe–O phase proposed by Pereira [9]. Furthermore, the peaks of the Fourier-transformed $\chi(k) \times k^3$ functions after the 1.3 V discharge has similar peak features to metal iron. These results show traces of the conversion reaction of FeOF to Fe, LiF and Li_2O. It appears to begin to react in voltage range between 1.8 and 1.3 V. K. M. Wiaderek and co-author also proposed that FeO_xF_{2-x} nanocomposite discharged down to 1.5 V was composed of $Li_xFe_yO_z$, Fe and LiF [11].

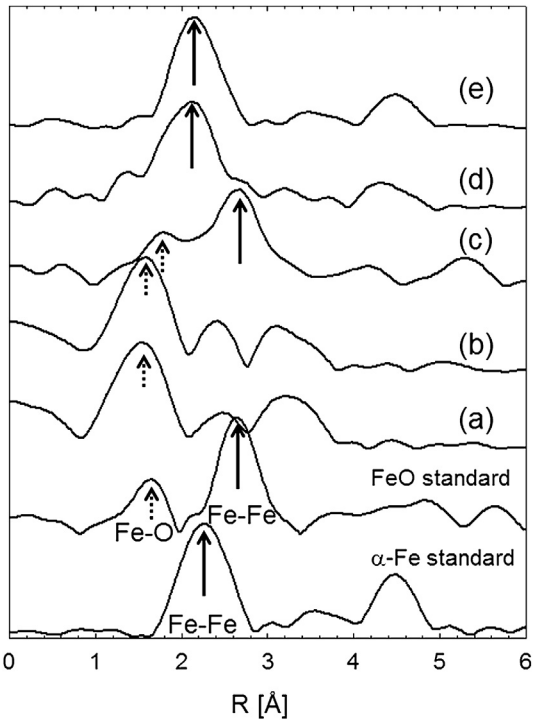

Fig. 9. Fourier transformation of the $\chi(k) \times k^3$ functions of FeOF cathode pellets during the first discharge/charge cycle; (a) initial FeOF state, (b) discharged pellet down to 2.0 V, (c) 1.8 V, (d) 1.3 V and (e) 0.7 V, respectively.

According to these consistent results from the XRD, EXAFS and XPS measurements, the discharge–charge reaction for FeOF progresses by the following reactions:

$$Fe^{3+}OF + Li \rightarrow LiFe^{2+}OF \quad (2)$$

$$LiFe^{2+}OF + 2Li \rightarrow LiF + Li_2O + Fe^0 \quad (3)$$

4. Conclusions

A novel synthesis method for FeOF has been developed using the roll-quenching method. The composition of obtained FeOF was $FeO_{1.1\pm1}F_{0.97}$ and it showed an excellent reversible capacity of 550 mAh g^{-1}, corresponding to 1.8 Li per FeOF. The larger capacity more than 1 Li per FeOF must be caused by a conversion reaction, because it can't be explained by Li insertion based on Fe^{3+}/Fe^{2+} redox reaction. However, the discharge capacity at the 30th cycle remained at 350 mAh g^{-1} at the voltage range between 1.3 and 4.0 V. Usually, the reversibility of the conversion reaction is poor, because of the large volume change of the active material. It is noteworthy that the cyclability is much better than that of the other conversion-type cathodes such as FeF_3 or Fe_2O_3. Although the average discharge voltage is as low as 2 V, the obtained FeOF has exceedingly high energy density 1100 mWh g^{-1} at rate of 10 mA g^{-1}. Moreover, the energy density of obtained FeOF at rate of 60 mA g^{-1} is equivalent to that of $LiFePO_4$.

Acknowledgments

This work was financially supported by the Research & Development Initiative for Scientific Innovation of New Generation Batteries (RISING project) of the New Energy and Industrial Technology Development Organization (NEDO), Japan. Fe K-edge XANES measurements at BL11 were conducted with help of Dr. Ryota Otani and Dr. Toshihiro Okajima of Kyushu Synchrotron Light Research Center.

References

[1] J.W. Choi, G. Cheruvally, H.J. Ahn, K.W. Kim, J.H. Ahn, J. Power Sources 163 (2006) 158.
[2] P. Poisot, S. Laruelle, S. Grugeon, J.-M. Tarascon, J. Electrochem. Soc. 149 (2002) A1212.
[3] Y. Idota, T. Kubota, A. Matsufuji, Y. Maekawa, T. Miyasaka, Science 276 (1997) 1395.
[4] M. Nishijima, I.D. Gocheva, S. Okada, T. Doi, J. Yamaki, T. Nishida, J. Power Sources 190 (2009) 558.
[5] F. Badway, F. Cosandey, N. Pereira, G.G. Amatucci, J. Electrochem. Soc. 150 (2003) A1318.
[6] F. Badway, A.N. Mansour, N. Pereira, J.F. Al-Sharab, F. Cosandey, I. Plitz, G.G. Amatucci, Chem. Mater. 19 (2007) 4129.
[7] H. Arai, S. Okada, Y. Sakurai, J. Yamaki, J. Power Sources 68 (1997) 716.
[8] F.J. Brink, R.L. Withers, J.G. Thompson, J. Solid State Chem. 155 (2000) 359.
[9] N. Pereira, F. Badway, M. Wartelsky, S. Gunn, G.G. Amatucci, J. Electrochem. Soc. 156 (2009) A407.
[10] M.C. Biesingera, B.P. Payne, A.P. Grosvenor, L.W.M. Lau, A.R. Gerson, R.St.C. Smart, Appl. Surf. Sci. 257 (2011) 2717.
[11] K.L. Wiaderek, O.J. Borkiewicz, E. Castillo-Martinez, R. Robert, N. Pereira, G.G. Amatucci, C.P. Grey, P.J. Chupas, K.W. Chapman, J. Am. Chem. Soc. 135 (2013) 4070.